Journal of Solid State Chemistry 187 (2012) 149–158

Contents lists available at SciVerse ScienceDirect

Journal of Solid State Chemistry

journal homepage: www.elsevier.com/locate/jssc

Structural differences of metal biphenylenebisphosphonate with change in the alkali metal

Tiffany L. Kinnibrugh, Nancy Garcia, Abraham Clearfield *

Department of Chemistry, Texas A&M University, P.O. Box 30012, College Station, TX 77842, USA

ARTICLE INFO

Article history:
Received 11 October 2011
Received in revised form
8 December 2011
Accepted 26 December 2011
Available online 4 January 2012

Keywords:
Layered compounds
Pillared solids
Potential Brönsted acid catalysts

ABSTRACT

A series of monovalent biphenylenebisphosphonates have been prepared using hydrothermal synthesis resulting in a composition $M[HO_3PC_{12}H_8PO_3H_2]$ where $M=Li^+$, Na^+, K^+, Rb^+, and Cs^+. Three of the original four phosphonic acid protons are retained, making the compounds Brönsted acids. A synthesis using microwave irradiation results in a new compound, $Na_2(HO_3PC_{12}H_8PO_3H)$, where only two protons are retained. Two structural types were found for the three-dimensional compounds where one type has a continuous inorganic layer. In the other structural type, the inorganic layer is formed by hydrogen bonding between neighboring chains. These structural variations arise as the coordination number changes from 4 for lithium to 8 for cesium without change in composition. The dense packing of the biphenylenebisphosphonate restricts the access to the protons, thus these compounds cannot be used as Brönsted acid catalysts. Alternatively, addition of N,N-dimethylformamide to the reaction mixture results in inclusion of ammonium ions in the cavities.

1. Introduction

Metal phosphonate chemistry is an ever-expanding discipline which had its beginning in 1978 with the synthesis of a family of zirconium phosphonates [1]. Extensive work has now been reported on the broad sampling of divalent, trivalent, and tetravalent cations [2–6]. However, very little has been reported on phosphonates of monovalent ions [7–10]. Recently, Rao and Vidyasagar [9] reported on the series of group 1 phenyl phosphonates. The general formula for this group of compounds is $M(HO_3PC_6H_5)(H_2O_3PC_6H_5)$. All the compounds are layered except lithium which has the same composition but form one-dimensional chains. The intriguing aspect of these compounds is that one of the phosphonate ligands retains both the protons yet bonds to the metal ions by chelation. Another interesting aspect of these compounds is that they have three protons for every metal ion. This makes Brönsted acids that are able to intercalate amines [9]. No structures of the amine intercalates were reported. It should also be mentioned that there are three different structures among the five alkali metal phenyl phosphonates. The principal driving force for the change in structure appears to be the increase in the size of the alkali metal ions.

Subsequently, the same authors prepared derivatives of the alkali metal ions with ethylene diphosphonate, $H_2O_3PC_2H_4PO_3H_3$ [10]. Interestingly, the products are three-dimensional of composition $M[HO_3PC_2H_4PO_3H_2]$, retaining three protons per alkali cation. The authors envision these compounds as strong Brönsted acids. Indeed, these phosphonates do intercalate and deintercalate ammonia. Of the seven such compounds prepared, thalium and ammonium along with the five alkali cations, four structure types were found. A different type of three-dimensional compound was formed from the monocarbondiphosphonic acid, $Na(HO_3PCH_2PO_2H_2)_n$ [8].

Our interest lies in whether these compounds can be prepared in porous form. If the pores were uniform, they would be lined with protons that could act as Brönsted acid catalysts, as an ion exchanger, and as base intercalation media. The unlikelihood of this porous form is attributed to the expected high solubility of such compounds due to the ionic nature of the cations. However, one may not have expected that the alkali metal ions would form supramolecular chains and layers rather than single molecular compounds with displacement of the protons by the metal ions forming strictly ionic species. One possible method of decreasing the solubility is to crosslink the layers into three-dimensional compounds with highly hydrophobic groups.

2. Materials and methods

All commercially available reactants ($LiNO_3$ Aldrich, $NaCO_3 \cdot H_2O$ 99.5% Baker Analyzed, K_2CO_3 99% EMD, Rb_2CO_3 99% and Cs_2CO_3 99% Alfa Aesar were used as purchased without further purification unless specified. Toluene was dried on 3 Å

* Corresponding author. Fax: +1 979 845 2370.
E-mail addresses: tkinnibrugh@mail.chem.tamu.edu (T.L. Kinnibrugh), clearfield@mail.chem.tamu.edu (A. Clearfield).

0022-4596/$ - see front matter © 2012 Elsevier Inc. All rights reserved.
doi:10.1016/j.jssc.2011.12.034

molecular sieves. Biphenylenebisphosphonic acid was synthesized according to previous methods [11].

2.1. Pillared materials

2.1.1. Hydrothermal synthesis of $Li(HO_3PC_{12}H_8PO_3H_2)$, compound **1**

The hydrothermal reaction for lithium was carried out at 160 °C for 5 days with a 1:1 ratio of 4,4′-biphenylenebisphosphonic acid (0.6 mmol, 0.1886 g) to lithium nitrate (0.6 mmol, 0.0828 g) in 5 mL of DI water. The reaction was carried out in a PTFE-lined pressure vessel of 12 mL capacity resulting in a white powder. The reaction resulted in a 74% yield based on the starting amount of ligand. Starting with the resulting powder (0.143 g), a further hydrothermal reaction was carried out at 180 °C in 4 mL water for 1 week to obtain single crystals. ICP-AES analysis gave a P/M ratio of 2.1.

2.1.2. Hydrothermal synthesis of $M(HO_3PC_{12}H_8PO_3H_2)$, compounds **2–5**

The hydrothermal reactions for cations sodium through cesium were carried out at 145 °C for 7 days with 1:1 ratio of 4,4′-biphenylenebisphosphonic acid (0.05 mmol, 0.0158 g) to metal carbonate (0.05 mmol) in 6 mL DI water. All reactions were carried out in a PTFE-lined pressure vessel of 12 mL capacity. The reactions resulted in single crystals for all cations. Larger reactions with the same cations (4,4′-biphenylenebisphosphonic acid (0.6 mmol, 0.1884 g)) were carried out at 180 °C for 3 days in 5 mL of DI water with an expected 50% yield. The compounds were then washed with ethanol and dried in an oven at 65 °C overnight. [Yields based on the starting amount of ligand for compounds **2–5,** respectively: 23.9%, 13.4%, 15.5%, 17.9%.] The yields were low due to solubility of the product. Slow evaporation of the products results in higher yields but are contaminated with reactants. Electron microprobe analysis gave P/M ratios of 1.8, 1.8, 1.9, and 2.1 for compounds **2**–**5**, respectively.

2.1.3. Microwave synthesis of $Na_2(HO_3PC_{12}H_8PO_3H)$, compound **6**

An CEM Explorer® 12 Hybrid microwave was used for the microwave synthesis. Reactions with a 1:1 ratio of 4,4′-biphenylenebisphosphonic acid (0.15 mmol, 0.0458 g) and sodium carbonate (0.15 mmol, 0.0186 g) were heated at 145 °C in 1 mL of water for 7 h using microwave radiation (average 18 W, max. 50 W). The product was washed with ethanol and dried in an oven at 65 °C overnight. A similar reaction was run for cesium biphenylenephosphonate resulting in compound **5**. Single crystals were obtained only for the cations sodium (**6**) and cesium (**5**). [55% yield based on the starting amount of ligand]. Electron microprobe analysis gave a P/M ratio of 0.9.

2.1.4. Synthesis of $Na_2(O_3PC_{12}H_8PO_3H)(H_2NC_2H_6)(H_2O)_8$, compound **7**

The solvothermal reaction was carried out in 5 mL of dry toluene, 60 μL of DI water, 0.0106 g (0.086 mmol) $Na_2CO_3 \cdot H_2O$, 0.0166 g (0.05 mmol) 4,4′-biphenylenebisphosphonic acid hydrate, and 60 μL dimethylformamide and heated for 7 days at 120 °C. The reaction was carried out in a PTFE-lined pressure vessel of 12 mL capacity. A single crystal was selected from the mother liquid.

2.2. Characterization

Powder XRD patterns were recorded using a Bruker D8-Focus Bragg-Brentano X-ray powder diffractometer (Cu$K\alpha$ radiation, $\lambda = 1.5418$ Å) operating at room temperature. Single crystal data was collected on a Bruker-AXS Apex II CCD X-ray diffractometer (Mo$K\alpha$ radiation, $\lambda = 0.71073$ Å) operating at 110 K. The structures were solved by direct methods and refined by the full-matrix least-squares technique against F^2 with the anisotropic displacement parameters for all non-hydrogen atoms. Hydrogen atoms were added in idealized positions and refined using a riding model with $U_{iso} = nU_{eq}$ for carbon atoms connected to the relevant H-atom where $n = 1.5$ for methyl and $n = 1.2$ for other H-atoms except compound **6**. Hydrogen atoms on water molecules and amine nitrogen were found using a Patterson map and refined using a riding model with $U_{iso} = nU_{eq}$ where $n = 1.5$ except for two water molecules in compound **7**. Anisotropic displacement parameters were established for all non-hydrogen atoms. The following programs were utilized: cell refinement and data reduction: SAINT[12]; semi-empirical method for absorption correction: SADABS[13]; structure solution: SHELXTL[14]; molecular graphics: ORTEPII[15], Mercury[16].

Thermogravimetric analysis (TGA) was performed under airflow from room temperature to 1000 °C with a heating rate of 10 K min^{-1} on a TGA Q500 apparatus. An additional TGA for compound **1** was also performed under similar condition but instead under nitrogen gas flow. Surface area measurements were performed on an Autosorb-6 (Quantachrome) unit using nitrogen and hydrogen adsorption at liquid nitrogen temperature. Samples were pre-calcined at 150 °C overnight and then degassed at 180 °C for 20 h. The data were analyzed using the software supplied by the Quantachrome Corporation and surface areas were calculated based on the Brunauer–Emmett–Teller (BET) model.

For elemental analysis of the compounds, both ICP and electron microprobe techniques were used. Quantitative compositional analyses for compounds **2**–**6** were carried out on a four spectrometer Cameca SX50 electron microprobe at an accelerating voltage of 15 kV at a beam current of 10 nA. All quantitative work employed wavelength-dispersive spectrometers (WDS). Analyses were carried out after standardization using well-characterized compounds or pure elements. Qualitative analyses (spectra) were obtained with an Imix Princeton Gamma Tech (PGT) energy dispersive system (EDS) using a thin-window detector. To prepare the samples for ICP-AES at Anderson Analytical, 0.0110 g of compound **1** was dissolved in 20 μL of conc. HCl and 20 mL of DI water which then was shaken over night.

3. Results

We have hydrothermally synthesized and structurally characterized five monovalent metal (M^+ = Li, Na, K, Rb, Cs) 4,4′-biphenylenebisphosphonates, $M(HO_3PC_{12}H_8PO_3H_2)$, **1**–**5**, with three-dimensional structures. The resulting compounds have a 1:1 ratio of metal to ligand, but a 1:2 ratio to the phosphonic acid groups. In concert with the previous publications [9,10], the retention of three of the original four protons of the ligand imparts Brönsted acidity to these compounds. Crystallographic data for the five compounds are presented in Table 1. All of the compounds are three-dimensional including the lithium compound which formed linear chains as the phenylphosphonate. In addition to these five compounds, a second sodium derivative (compound **6**) was prepared utilizing microwave radiation and a third more potentially porous version was prepared by addition of an amine as a reactant (compound **7**).

3.1. Crystal structure descriptions

Although the values of the triclinic unit cell parameters are similar for compounds **2–5,** several different structural types were found. Each centrosymmetric triclinic unit cell has two unit formulas per unit cell while the centrosymmetric monoclinic unit cells for compounds **1** and **6** have four unit formulas present.

Table 1
Crystallographic data, details of data collection and refinement.

	1	2	3	4	5	6	7
Formula	$Li(HO_3PC_{12}H_8PO_3H_2)$	$Na(HO_3PC_{12}H_8PO_3H_2)$	$K(HO_3PC_{12}H_8PO_3H_2)$	$Rb(HO_3PC_{12}H_8PO_3H_2)$	$Cs(HO_3PC_{12}H_8PO_3H_2)$	$Na_2(HO_3PC_{12}H_8PO_3H)$	$Na_2(H_2O)_7(O_3PC_{12}H_8PO_3)(H_2N(CH_3)_2)_2\cdot H_2O$
M_r	320.09	336.14	352.25	398.62	446.06	358.12	547.33
Crystal color, habit	Colorless, plate	Colorless, plate	Colorless, plate	Colorless, plate	Colorless, plate	Colorless, plate	Colorless, plate
Crystal size (mm^3)	$0.20\times0.09\times0.02$	$0.25\times0.20\times0.03$	$0.22\times0.15\times0.03$	$0.36\times0.24\times0.04$	$0.21\times0.05\times0.03$	$0.20\times0.16\times0.02$	$0.25\times0.20\times0.03$
T(K)	110	110	110	110	110	110	110
Crystal system	Monoclinic	Triclinic	Triclinic	Triclinic	Triclinic	Monoclinic	Triclinic
space group	*C* 2/*c*	*P*-1	*P*-1	*P*-1	*P*-1	*C* 2/*c*	*P*-1
a (Å)	27.368(3)	5.716(4)	5.879(5)	5.872(2)	6.1734(4)	28.28(2)	8.369(3)
b (Å)	8.6016(9)	7.905(6)	7.778(7)	7.680(3)	7.5322(5)	7.547(6)	9.522(5)
c (Å)	5.4046(6)	14.366(10)	15.134(13)	15.242(5)	15.3998(10)	6.390(6)	16.5383(15)
α (°)	90.00	88.100(8)	79.077(12)	101.822(3)	102.2190(11)	90.00	78.33(4)
β (°)	98.025(2)	84.499(8)	86.606(11)	91.516(4)	94.2830(10)	101.26(2)	83.71(3)
γ (°)	90.00	82.628(7)	85.822(12)	93.709(4)	94.3050(10)	90.00	72.19(4)
V ($Å^3$)	1259.8(2)	640.6(8)	676.9(10)	670.8(4)	694.86(8)	1337.6(19)	1227.2(8)
Z	4	2	2	2	2	4	2
ρ_{calc} ($g\,cm^{-3}$)	1.688	1.743	1.728	1.974	2.132	1.778	1.481
2θmax(°)	58.2	52.8	54.7	52.0	58.4	57.0	57.8
μ(Mo$K\alpha$) (cm^{-1})	0.369	0.398	0.653	3.953	2.919	0.416	0.278
Min/max trans factors	0.9312/0.9936	0.9059/0.9897	0.8697/0.9807	0.3342/0.8579	0.5793/0.9175	0.9196/0.9917	0.9329/0.9928
Total reflections	9331	6252	7780	5184	14177	9347	14440
Unique reflections	1607	2486	3065	2379	3333	1692	5802
Observed reflections $[I>2\sigma(I)]$	1438	1313	2121	2590	3115	1383	4747
$R_1/\omega R_2$	0.0307/0.1183	0.0725/0.1513	0.0409/0.0922	0.0261/0.0645	0.0288/0.0763	0.0337/0.0868	0.0442/0.1235
No. of parameters	96	184	190	191	190	121	373
S	1.059	1.014	1.002	1.054	1.055	1.035	1.094
Diff. density max/min	0.439/−0.406	0.846/−0.599	0.497/−0.423	0.454/−0.405	1.956/−1.874	0.468/−0.388	0.822/−0.547

Table 2
Bond distances for the five biphenylenephosphonates (Å).

Compounds	1	2	3	4	5
M–O	O1 1.932(2) O1A 1.963(2)	O1 2.437(5) O2 2.485(5) O3 2.432(4) O4 2.478(5) O5 2.287(5) O5D 2.340(5)	O1 2.756(3) O2 2.704(3) O3 2.926(3) O4 2.699(3) O5 2.710(3) O6 2.812(3)	O1 2.865(2) O2 2.861(2) O3 2.946(2) O4 2.980(2) O5 2.819(2) O6 3.178(2) O6 3.220(2)	O1 3.220(2) O2 3.067(2) O3 3.090(3) O3C 3.284(2) O4 3.065(3) O4B 3.331(3) O5 3.340(3) O6 3.321(3)
M–O[a]			O3 3.322(3) O4 3.297(3)	O2 3.396(2)	O2 3.430(3) O5 3.410(2)
P1–O1	1.494(1)	1.499(4)	1.556(2)	1.533(2)	1.558(2)
P1–O2	1.563(1)	1.541(4)	1.493(2)	1.496(2)	1.503(2)
P1–O3	1.542(1)	1.554(4)	1.554(2)	1.547(2)	1.527(2)
P2–O4		1.592(4)	1.523(2)	1.511(2)	1.505(3)
P2–O5		1.476(4)	1.562(2)	1.504(2)	1.529(3)
P2–O6		1.542(4)	1.510(2)	1.566(2)	1.563(3)

[a] Long interactions.

The monoclinic unit cell parameters found for compounds **1** and for $Li(HO_3PC_2H_4PO_3H_2)$ [10] doubles the *a*-axis, thereby including two layers in the unit cell. The sodium phenylphosphonate compound synthesized by Rao and Vidasagar [9] has similar unit cell parameters to our compound **2**, except the *c*-axis is slightly longer. This is attributed to the van der Waals gap between the layers of sodium phenylphosphonates, whereas in compound **2** the phenyl groups are connected. Structural similarities for compounds **2**–**5** have the M^+ ions approximately confined to the *ab* plane. The inorganic planes (MO_nP_m) are separated by hydrophobic regions of biphenylene groups and the oxygen atoms of phosphonates coordinate to the M^+ ions on both sides of the plane. Compounds **1** and **6** are similar except M^+ ions are approximately confined to the *bc* plane instead of the *ab* plane, because of the choice of their *a*-axis. The bond lengths (Table 2) are similar to those of reported structures [8–10] in the literature. The labeling scheme for the 4,4′-biphenylenebisphosphonate utilized here is given in Fig. 1.

3.2. Crystal structure of $Li(HO_3PC_{12}H_8PO_3H_2)$, compound *1*

The lithium atom in compound (**1**) has half-occupancy in the unit cell and is tetrahedrally bonded to oxygen atoms (O1 and O1A) of four phosphonate moieties as shown in Fig. 2. Each

tetrahedron (LiO_4) shares an edge with two other tetrahedra forming chains along the *c*-axis (Fig. 2a). The metal oxygen bonds are given in Table 2 with the longer bonds represented by a dashed line in Fig. 2a. The oxygen atoms O2 and O3 are not involved in metal oxygen bonding. The P–O bond lengths can indicate the degree of protonation of the oxygen atoms and are given in Table 2. The P–O bond lengths indicate that the unbonded oxygen atoms bear the protons with atom O2 fully protonated and O3 partially protonated. The partial protontation of O3 is due to the half-occupancy of the lithium atom in the unit cell. The chains stack along the *b*-axis and terminate with O–H groups. Thus, hydrogen bonding within the chain (O3–H…O3) and across to neighboring chains (O2–H…O3) is observed (Table 3) forming a weak inorganic layer. The chains are linked together along the *a*-axis by diphosphonic acids forming a three-dimensional structure as seen in Fig. 2b.

3.3. Crystal structure of $Na(HO_3PC_{12}H_8PO_3H_2)$, compound **2**

The sodium compound (**2**) has an edge-shared bioctahedral Na_2O_{10} motif, formed from 10 different phosphonate moieties (Fig. 3). Each sodium atom in the Na_2O_{10} unit is six-coordinate and bonded to six different phosphonate moieties, thus no chelation is observed. The oxygen atom O6 does not bond to any metal atoms, instead it forms hydrogen bonds to O2–H and O3–H (Table 3). Each octahedron shares one edge (O5 and O5D) resulting in the edge-shared bioctahedral, Na_2O_{10}, which is corner-connected to eight symmetry equivalent bioctahedra, together forming an inorganic layer in the *ab*-plane (Fig. 3a). The layers stacked along the *c*-axis, have an interlayer distance of 14.94 Å. Each inorganic layer has alternating four- and eight-membered rings along the *b*-axis. The diphosphonates, in **2**, cross-links the inorganic layer together forming a regular pillared structure (Fig. 3c). Interestingly, neighboring pillars along the a*b*-diagonal are rotated 54° from each other presumably to reduce strain caused by close contacts from other neighboring pillars (Fig. 3b). Noteworthy, the potential C–H..π distances (shortest C-H..π 3.696 Å, 127 °C) are longer than the van der Waals radii.

3.4. Crystal structure of $K(HO_3PC_{12}H_8PO_3H_2)$, compound **3**

The potassium compound (**3**) consists of six-coordinate metal atoms with the K–O bond distances ranging from 2.699(3) to 2.926(3) Å (K1–O3) as shown in Fig. 4a and Table 2. The average bond distance is 2.768 Å, which is in agreement with the sum of the ionic radii [17]. Six different phosphonate moieties are bonded to each octahedral potassium atom, three above and three below to form a trigonal prism arrangement. All three oxygen atoms of each phosphonate group are bonded to three different potassium atoms forming chains running long the *a*-axis as shown in Fig. 4b. In the figure the oxygen atoms are seen to bridge across potassium ions. The diphosphonates cross-link the chains as shown in Fig. 4c. We note that in the *b* direction the chains terminate with O–H bonds where the shortest metal oxygen distance between neighboring chains is 3.753 Å.

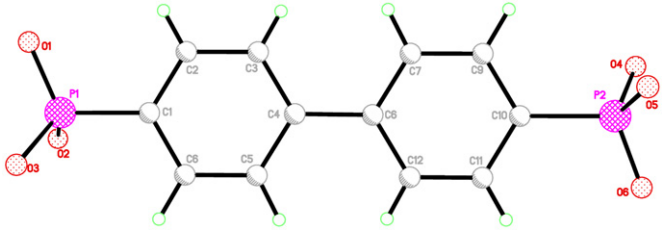

Fig. 1. Labeling scheme for biphenylenediphosphonate.

Table 3
Hydrogen bond distances for several of the alkali metal phosphonates.

Compound	O–H…O	Bond length (Å)	Symmetry
1	O2–H…O3	2.629(1)	$x, 2-y, -½+z$
	O3–H…O3	2.434(2)	$-x, y, ½-z$
2	O2–H…O6	2.561(5)	$1+x, -1+y, z$
	O3–H…O6	2.509(6)	$x, -1+y, z$
3	O1–H…O6	2.468(3)	$-x, 1-y, -z$
	O5–H…O2	2.546(4)	$-1-x, 1-y, -z$
4	O3–H…O5	2.471(3)	$-x, 1-y, 1-z$
	O4–H…O1	2.414(3)	$1-x, 1-y, 1-z$
6	O3–H…O2	2.572(2)	$x, 1-y, ½+z$

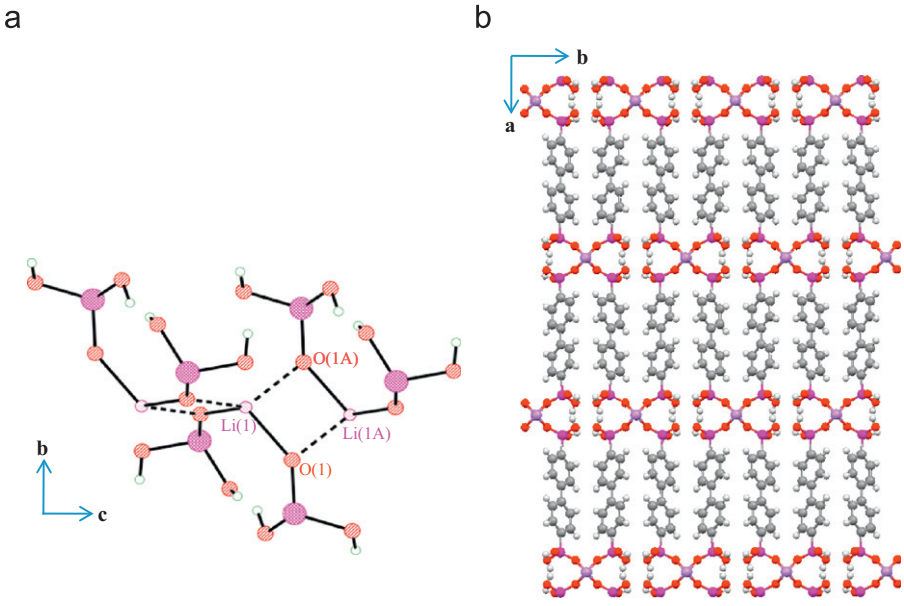

Fig. 2. Metal oxygen chain showing the perpendicular 4-membered rings (a) and the crystal packing of compound **1** as viewed down the *c*-axis (b).

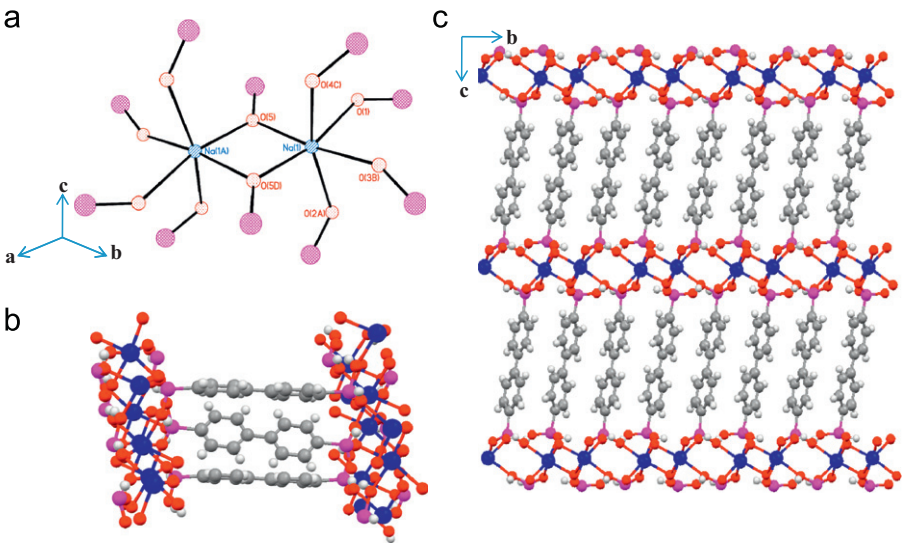

Fig. 3. The Na_2O_{10} dimer (a), neighboring pillars along the a*b*-diagonal (b), and crystal packing (c) of compound **2** as viewed down the *a*-axis.

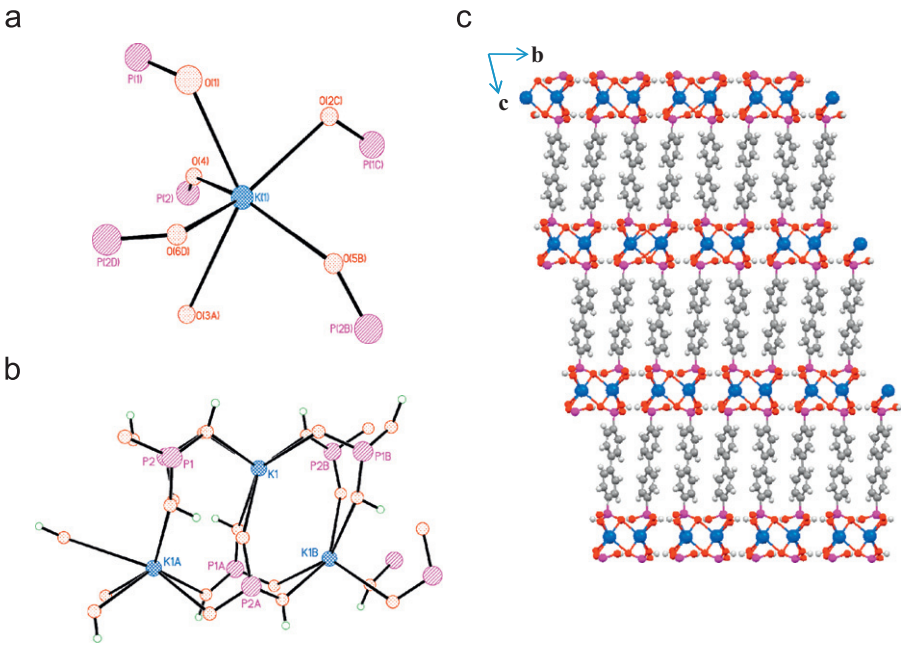

Fig. 4. Numbering scheme (a), top view of the chain made from corner connected octahedra (b), and crystal packing (c) for compound **3**.

The inorganic layer is formed from hydrogen bonding between neighboring chains (Table 3). The biphenylene groups are rotated relative to each other by 54° as shown in Fig. 3b for the sodium structure.

3.5. Crystal structure of $Rb(HO_3PC_{12}H_8PO_3H_2)$, compound **4**

The rubidium atom is seven coordinate due to a chelating group (O5–P2–O6) and five additional bonds each from a different phosphonate group (Fig. 5a). Two such Rb ions are bridged together by O3–P1–O2 phosphonate groups as shown in Fig. 5b to form 8-membered rings. The Rb….Rb distance is 4.18 Å and this is close enough that O6c and O6a each donate an electron pair to an adjacent Rb atom to form a four-membered ring within the 8-membered ring. The P2–O bond distances to Rb in the chelate group are 2.819(2) for O5a and 3.178(2) Å for O6a. The donated bond P2–O6c is 3.220(2) Å. The motif shown in Fig. 5b is an Rb_2O_{12} unit that then propagates by corner connections to form chains running along the *a* direction. The chains terminate along the *b*-axis with O–H groups where the shortest metal oxygen distance between neighboring chains is 3.518 Å. Hydrogen bonding occurs between chains building a weak inorganic layer, reducing the potential pore size in half (Table 3). As with the potassium compound, the Rb_2O_{12} units are cross-linked by the biphenylenebisphosphonates (Fig. 5c) in the *c* direction. Similar to both compounds **1** and **3**, the biphenylenebisphosphonates cross-link the chains along the *c*-axis and neighboring pillars along the *ab*-diagonal are rotated 60° from each other.

3.6. Crystal structure of $Cs(HO_3PC_{12}H_8PO_3H_2)$, compound **5**

The cesium compound (**5**) has Cs^+ in an 8-coordinate distorted dodecahedral polyhedron (Fig. 6a). The chelating atoms O4 and O5 have bond distances 3.065(3) and 3.340(3) Å, respectively. The O4 atom that chelates the Cs^+ ion then donates to a neighboring Cs^+ ion forming a four-membered ring. In addition,

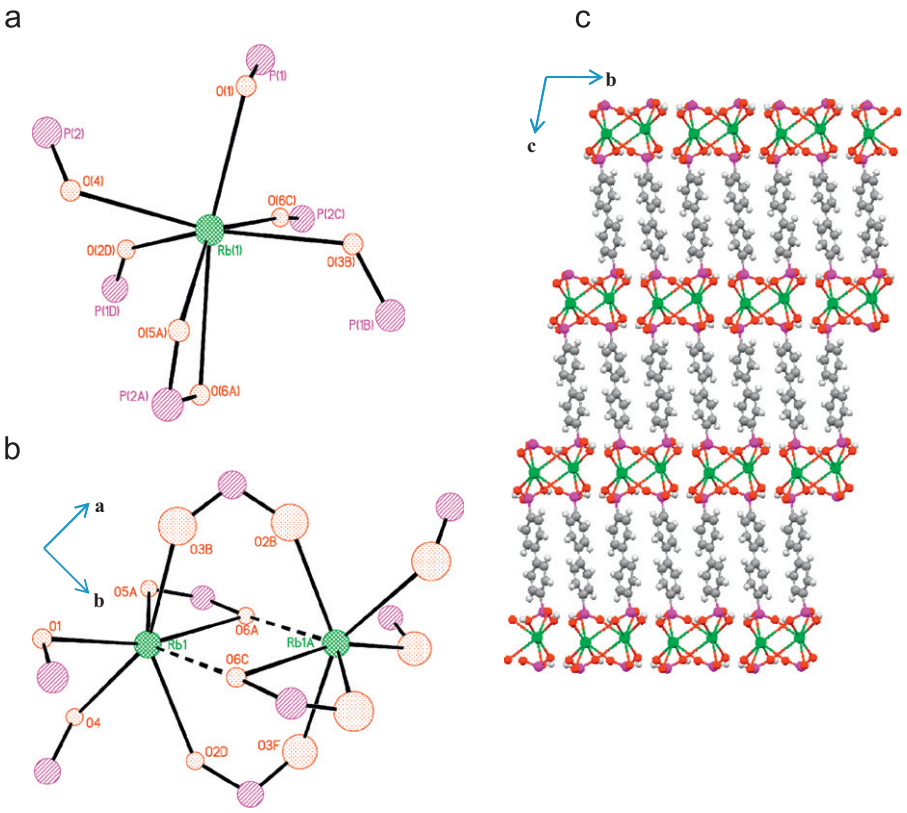

Fig. 5. Numbering scheme (a), dimer Rb_2O_{12} where the dashed lines indicate longer bonds (b), and crystal packing (c) for compound **4**.

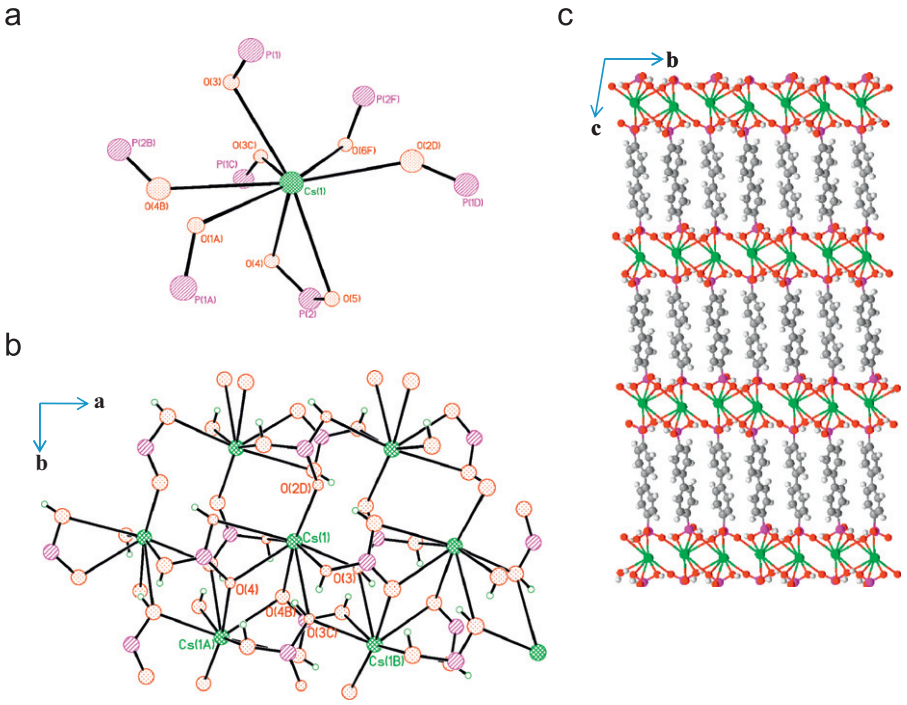

Fig. 6. Numbering scheme (a), top view of the metal layer built from chains of edge-shared dodecahedra linked together by O–P–O bridges (b), and crystal packing of compound **5** as viewed down the *a*-axis (c).

another four-membered ring is formed by O3 atoms from separate phosphonate groups (Fig. 6b). The parallel Cs^+ ions bridged together by two different four-membered rings in the *a* direction are then connected in the *b* direction by O2–P1–O1 and O2–P1–O3 forming a continuous layer with no gaps between rows (Fig. 6b). Similar to compound **2**, the inorganic layers are cross-linked by diphosphonates forming a regular pillared structure where pillars are rotated 54° from each other.

3.7. Crystal structure of $Na_2(HO_3PC_{12}H_8PO_3H)$, compound **6**

The microwave synthesis resulted in a regular pillared structure formed when layers are cross-linked by the biphenylenebisphosphonates for compound **6**, but the inorganic layers differ from that of compound **2**. There are two symmetry-independent sodium atoms (Na1 and Na2) each with half-occupancy in the unit cell. Each Na^+ ion is bonded to four different phosphonate moieties resulting in a tetrahedral geometry. The 4-coordinate metal is based on consideration of the ionic radii [17] and valence bond sum [18] (Table 4). Oxygen atom O3 is fully protonated and does not bond to any sodium atom. The symmetry independent sodium atoms form an edge-shared dimer, Na_2O_6, where oxygen atoms O1D and O1E form the edge. The dimers are corner connected together by O1–P1–O2 bridges forming alternating four and eight membered rings along the *b*-axis as shown in Fig. 7a. Oxygen atom O3 is positioned above the 8-membered ring and hydrogen bonds to atom O2A (Table 3). Neighboring dimers in the *c*-direction share edges building the inorganic layer (Fig. 7b). Diphosphonate groups cross-link the inorganic layers along the *a*-axis (Fig. 8). As with previous structures, the neighboring biphenylene groups are rotated ~61° to each other but in the *bc*-direction.

Table 4
Bond distances for compound **6** (Å).

M–O	Na2–O1E	2.399(2)	Na1–O1E	2.293(2)
	Na2–O1D	2.399(2)	Na1–O1D	2.293(2)
	Na2–O2	2.315(2)	Na1–O1B	2.394(2)
	Na2–O2A	2.315(2)	Na1–O1F	2.394(2)
M–O[a]	Na2–O2	2.534(2)	Na1–O3	2.645(2)
	Na2–O2	2.534(2)	Na1–O3	2.645(2)
P1–O1	1.504(2)			
P1–O2	1.511(2)			
P1–O3	1.580(2)			

[a] Long M–O distances

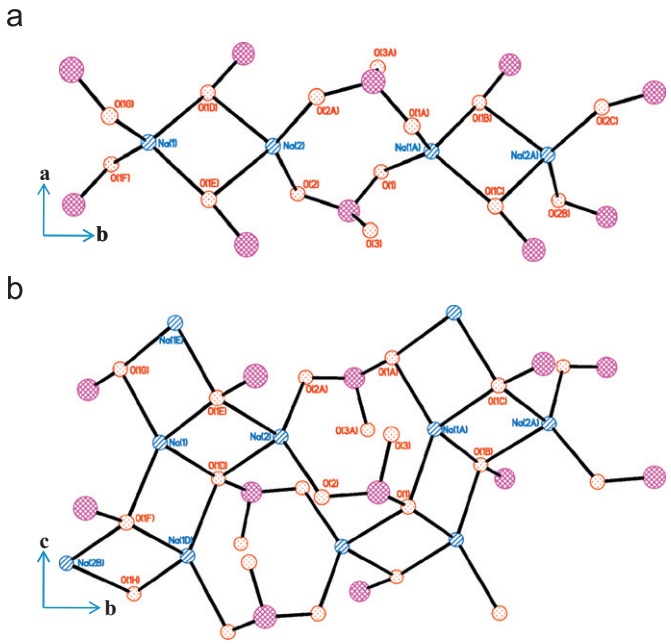

Fig. 7. Four- and eight-membered rings along the *b*-axis (a) and a view of the inorganic layer in the *bc*-plane (b) of compound **6**.

3.8. Crystal structure of $Na_2(O_3PC_{12}H_8PO_3H)(H_2NC_2H_6)(H_2O)_8$, compound **7**

A three-dimensional supramolecular structure was obtained from the addition of N,N-dimethyl formamide as a reactant (Fig. 9c). The structure consists of chains built from sodium atoms and water molecules (Table 5). Three symmetry independent sodium atoms were determined where two metal atoms are six-coordinate with an octahedral geometry and the third is a five-coordinate trigonal bipyramidal atom. The six-coordinate sodium atoms have half-occupancy in the unit cell. The chains have a zig-zag form where the five-coordinate metal atom is on the corner. The six-coordinate sodium atoms connect the corners together by forming four-membered rings with each five-coordinate sodium atom thus forming the zig-zag chains (Fig. 9a). The biphenylene diphosphonic acid molecules hydrogen bond (Table 6) to the chains (Fig. 9c) and free water molecules, forming cavities with dimensions 8.52 Å × 7.57 Å × 11.78 Å. Each cavity is filled with two dimethyl ammonium ions from decomposed DMF (Fig. 9b). Charge balance is achieved by a total negative three charge from the biphenylene diphosphonic acid molecule countered by two Na^+ ions and a dimethyl ammonium ion.

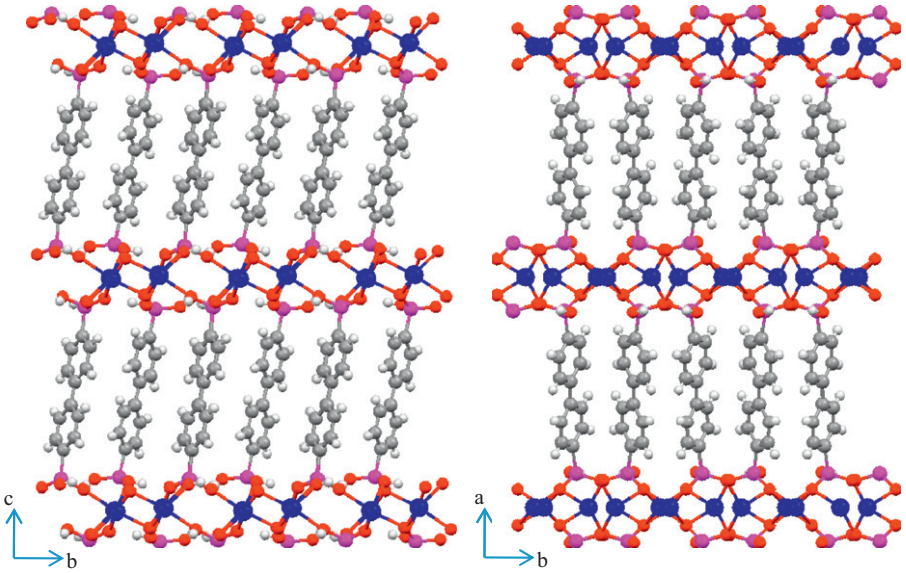

Fig. 8. Comparison of the crystal packing for compounds **2** (left) and **6** (right).

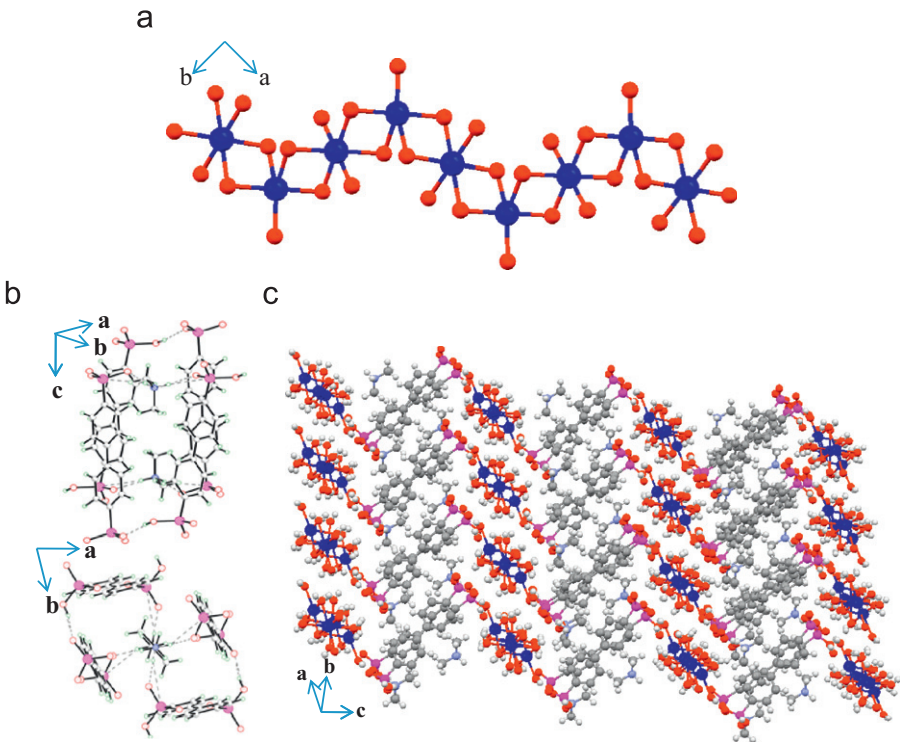

Fig. 9. View of the inorganic zig-zag chain (a) for compound **7**. Two perspectives of the cavity for compound **7** are presented, showing two dimethyl ammonium ions inside the cavity (b). Crystal packing of the supramolecular structure (c). The hydrogen bonding between the chains and the diphosphonic acids are not shown for clarity.

Table 5
Bond distances for compound **7** (Å).

Na1–O9	2.307(2)	Na2–O7A	2.356(2)	Na3–O13A	2.350(2)
Na1–O12	2.309(2)	Na2–O7B	2.356(2)	Na3–O13B	2.350(2)
Na1–O8	2.333(2)	Na2–O8A	2.405(2)	Na3–O10A	2.382(2)
Na1–O10	2.406(2)	Na2–O8B	2.405(2)	Na3–O10B	2.382(2)
Na1–O7	2.735(2)	Na2–O11A	2.454(2)	Na3–O9A	2.410(2)
		Na2–O11B	2.454(2)	Na3–O9B	2.410(2)
P1–O1	1.518(2)				
P1–O2	1.528(2)				
P1–O3	1.530(2)				
P2–O4	1.497(2)				
P2–O5	1.569(2)				
P2-O6	1.511(1)				

4. Discussion

An interesting result that arises from the structures of the five alkali metal ion biphenylenebisphosphonates is the fact that the coordination number of the ions increase from four for Li^+ to eight for Cs^+, but the composition in each case is the same. This feat is accomplished by first producing linear chains with tetrahedral coordination of the lithium ions utilizing two of the six oxygen atoms available per Li^+ with four being non-bonding. In the six-coordinate sodium structure, Na_2O_{10} dimers are formed by O5 and O5D bridging the two sodium ions with O6 being non-bonding. The motif is octahedral. The potassium structure also features a 6-coordinate metal with all the oxygen atoms bonding to the metal ions but the motif is trigonal prismatic. The rubidium structure attains a 7-coordinate polyhedron by chelation of one of the phosphonate groups with one of the oxygen atoms also donating to an adjacent metal ion. The coordination is a capped trigonal prism. An 8-coordinate Cs^+ is obtained by both chelation and donation from a neighboring O3 atom.

All compounds have three-dimensional supramolecular structures with similar orientation of the biphenylene groups where neighboring biphenylene groups are rotated ~54° from each other presumably to reduce strain caused by close contacts from other neighboring pillars. Compounds **2** and **5** have regularly pillared structure types whereby a continuous inorganic layer is formed. Similar extended structure types were found for compounds **1**, **3**, and **4**, where hydrogen bonding between the neighboring chains builds the inorganic layers. Interestingly, the distance between the neighboring chains decreased along the *b*-axis as the atomic radii increased from compounds **3** to **5**. This distance may be a reflection of the volume of the unit cell, where the volume decreases from compounds **3** to **4**. The volume was expected to increase from compounds **1** to **5**. In the cesium compound **5**, the distance between pillars is small enough for metal and oxygen atoms to bond, forming continuous inorganic layers.

The stability of the compounds may be thought to be low considering that these are monovalent metals surrounded by many oxygen atoms sharing the metal charge. On the contrary, TGA data showed that all compounds were stable up to approximately 300 °C (Supplementary data S1). This is approximately 50 °C more stable than the ligand alone [19]. This stability may be due to the three-dimensional structures that were formed and the coordination of the phosphonates to the metal atoms. TGA ran under air resulted in a colorless glass residue with weight loss occurring in several steps. The initial weight loss beginning at approximately 300 °C for all compounds is attributed to loss of water due to condensation of the phosphonate. The TGA of compound **1**, run with nitrogen, initially had a similar TGA curve where the compound is stable to approximately 300 °C, but began to deviate around 530 °C. It resulted in an amorphous black powder instead.

Noteworthy is the metal to phosphonic acid ratio may be altered by choice of synthetic route. Using microwave radiation resulted in the sodium compound **6**, for which a 1:1 metal to phosphonic acid ratio was obtained. However, using a conventional heating method resulted in a 1:2 ratio for compound **2**.

Table 6
Hydrogen bond distances for compound **7**.

O–H…O	Bond length (Å)	Symmetry	O–H…O	Bond length (Å)	Symmetry
O4…O1	2.561(2)	x, y, z	O11…O3	2.842(2)	$x, y-1, z$
O7…O6	2.738(2)	x, y, z	O12…O2	2.832(3)	$x, y-1, z$
O7…O13	2.791(3)	$-x+1, -y+1, -z+1$	O12…O6	2.744(2)	$x-1, y, z$
O8…O12	2.847(2)	$-x+1, -y, -z+1$	O13…O3	2.874(2)	$-x+1, -y+1, -z+1$
O8…O3	2.855(2)	$x, y-1, z$	O13…O14	2.710(2)	$-x+1, -y+1, -z+1$
O9…O1	2.749(2)	x, y, z	O14…O6	2.679(3)	$-x+2, -y+1, -z+1$
O9…O14	2.830(2)	$-x+1, -y+1, -z+1$	O14…O3	2.738(3)	$-x+2, -y+1, -z+1$
O10…O2	2.771(2)	$-x+1, -y+1, -z+1$	N1…O5	2.673(3)	x, y, z
O10…O11	2.866(2)	$-x+2, -y, -z+1$	N1…O2	2.721(3)	$x+1, y-1, z$
O11…O5	2.816(2)	x, y, z			

A similar result was reported for a barium phosphonate [20]. The structural differences may be due to a more uniform heat distribution when using microwave radiation. Even with the 1:1 ratio the materials are still a Brönsted acid with one acidic proton remaining per phosphonate group. A regular pillared structure is obtained for both compounds **2** and **6**, but they differ in both coordination number and inorganic layer type resulting in different pillaring effects as shown in Fig. 8.

Previously, reported structures of alkali phosphonates used two types of phosphonic acid groups: ethylene and phenyl phosphonic acids. The alkali metals lithium and sodium are very similar to our compounds. Both compounds $Li(HO_3PC_6H_5)(H_2O_3PC_6H_5)$ [9] and $Li(HO_3PC_2H_4PO_3H_2)$ [10] are similar to compound **1**, where the lithium atom is tetrahedrally bonded to oxygen atoms forming chains. The structure of $Li(HO_3PC_6H_5)(H_2O_3PC_6H_5)$ is a one-dimensional structure, conversely using a diphosphonic acid both compound **1** and $Li(HO_3PC_2H_4PO_3H_2)$ resulted in similar three-dimensional structures.

The sodium compound **2** has similar metal coordination as $Na(HO_3PC_2H_4PO_3H_2)$ [10] and $Na(HO_3PC_6H_5)(H_2O_3PC_6H_5)$ [9] with edge-shared bioctahedra, Na_2O_{10}. In compound **2**, the layers stacked along the *c*-axis, have an interlayer distance of 14.94 Å which is shorter than 15.59 Å [9] for compound $Na(HO_3PC_6H_5)(H_2O_3PC_6H_5)$ where there is no interdigitation or π–π stacking of the phenyl rings thus forming a van der Waals gap. As with $Na(HO_3PC_2H_4PO_3H_2)$ [10], the diphosphonic acid, in **2**, links the inorganic layer together forming a regular pillared structure.

Structural differences between our compounds and those previously reported were observed for alkali metals potassium to cesium. The reported structures for the potassium ion range from 6- to 8-coordinate if the maximum bond distance 3.073 Å is considered [7,9,10]. Interestingly, a different structural type was found for compound $K(HO_3PC_2H_4PO_3H_2)$ [10] than for our compound **3,** in that a traditional pillared structure is not formed. Rather, there is no distinct inorganic or organic layer. Similarly, both our compounds **4** and **5** differ from the ethylene analogs ($Rb(HO_3PC_2H_4PO_3H_2)$ and $Cs(HO_3PC_2H_4PO_3H_2)$) [10]. The differences in structural types may be due to flexibility and size of the ethylenediphosphonates.

Rao and Vidyasager [9] stated that K, Rb, and $Cs(HO_3PC_6H_5)(H_2O_3PC_6H_5)$ have similar layered structure types although in our study this differs slightly. Compounds **1**, **3**, and **4** have similar extended structure types as lithium ethylene diphosphonate [10], where hydrogen bonding between chains build the inorganic layer. The cesium compound **5** differs from **3** and **4** where a continuous inorganic layer is formed.

The structure of the materials will influence the access to the acidic protons. Interestingly, the alkali phenylphosphonates, where the compounds form layers, intercalated both ammonium ions and amines. Here, an increase in *d*-spacing is observed with increase in amine size suggesting that the layers move apart to accommodate the amines. In the three-dimensional case, to accommodate the amine the framework must have some porosity. Intercalation/deintercalation of NH_4^+ into $Li(HO_3PC_2H_4PO_3H_2)$ [10] was observed, thus indicating flexibility of structure. Less ammonium intercalation occurred for $Na(HO_3PC_2H_4PO_3H_2)$ [10]. Still less intercalation of ammonia was observed for the potassium to cesium versions suggesting less porosity. Our compounds have similar structures to the lithium and sodium ethylenediphosphonates. In the case of **1**, **3**, and **4**, they are similar to $Li(HO_3PC_2H_4PO_3H_2)$ where the largest uptake of ammonia occurred. Additionally, the inorganic layer is built from chains hydrogen bonded together. One may suggest that reducing hydrogen bonding between chains would result in porosity. Surface area measurements of compound **1** showed no internal porosity and very small surface area (nitrogen 4.12 and hydrogen 4.13 cc/g). For our compounds, due to their three-dimensional structure and the more rigid ligand, intercalation of amines is not possible. Materials with larger pores would be needed.

In our study, *in situ* synthesis with DMF resulted in a new supramolecular structure with cavities containing dimethyl ammonium ions (compound **7**). This compound differs from the pillared structures found in compounds **2** and **6,** since the phosphonate groups are not coordinated to the metal atoms. A pillared structure still exists, where the inorganic and organic layers are separate. The organic pillars are arranged around the dimethyl ammonium ions to form cavities. With this arrangement and coordination of the phosphonate groups with the metal atoms would provide a more stable compound with potential porosity. This may suggest a different approach to obtain porosity for these materials is possible, where amines are used as templates. Several examples of amines as templates or structure directing agents for metal phosphonates and phosphates have been reported in the literature [21–27]. It could be envisioned that different amines would result in different three-dimensional structures with the amine incorporated in the structure. Removal of the amines would form pores where access to the protons is possible. This approach is being pursued.

5. Conclusions

Six monovalent metal biphenylenebisphosphonates have been synthesized and their structures have been determined with retention of most of the original four protons of the ligand imparting Brönsted acidity to these compounds. Unfortunately, access to these protons is blocked; therefore new methods to obtain Brönsted acid catalysts with pores so the protons can be accessed are needed. The *in situ* synthesis with DMF led to a three-dimensional structure with cavities containing dimethyl ammonium ions, giving insight into alternative methods of obtaining porosity.

Supplementary information

Structural information derived from the crystal structure refinements have been deposited at the Cambridge Crystallographic Data Center (e-mail:deposit@ccdc.cam.ac.uk) with CCDC file numbers: 847117–847123.

Acknowledgments

Authors are thankful to Ray N. Guillemette from the Geology Department for the electron microprobe measurement and Boris G. Shpeizer from the Chemistry Department for surface area analysis. This work was supported by the PR-LSAMP Bridge-to-the-doctorate and the Robert A. Welch Foundation under Grant no. A0673 for which grateful acknowledgment is made.

Appendix B. Supplementary Information

Supplementary data associated with this article can be found in the online version at doi:10.1016/j.jssc.2011.12.034.

References

[1] G. Alberti, U. Costantino, S. Allulli, N. Tomassini, J. Inorg. Nucl. Chem. 40 (1978) 1113–1117.
[2] R.W. Buckley (Ed.), Solid State Chemistry Research Trends, Nova Science Publishers Inc., Portland, 2007.
[3] G.K.H. Shimizu, R. Vaidhyanathan, J.M. Taylor, Chem. Soc. Rev. 38 (2009) 1430–1449.
[4] A. Clearfield, Dalton Trans. 44 (2008) 6089–6102.
[5] G.K.H. Shimizu, J.M. Taylor, R. Vaidhyanathan, Macromol. Containing Met. Met.-Like Elem. 9 (2009) 125–179.
[6] A. Clearfield, J. Alloys Compd. 418 (2006) 128–138.
[7] C.N. Caughlan, H. Mazhar ul, Inorg. Chem. 6 (1967) 1998–2002.
[8] K.P. Rao, K. Vidyasagar, Acta Cryst. E 61 (2005) m1794–m1796.
[9] K.P. Rao, K. Vidyasagar, Eur. J. Inorg. Chem. (2005) 4936–4943.
[10] K.P. Rao, K. Vidyasagar, Eur. J. Inorg. Chem. (2006) 813–819.
[11] Z. Wang, J.M. Heising, A. Clearfield, J. Am. Chem. Soc. 125 (2003) 10375–10383.
[12] Bruker SAINTP+ for NT. Data Reduction and Correction Program v. 7.56; Bruker AXS, Madison, Wisconsin, USA, 2005.
[13] G.M. Sheldrick, SADABS-2008/1, Bruker/Siemens Area Detector Absorption Correction Program, Bruker AXS, Wisconsin, USA, 2008.
[14] G.M. Sheldrick, SHELXTL 2008/4 Structure Determination Software Suite, SHELXTL 2008/4, Madison, Wisconsin, USA, 2008.
[15] C.K. Johnson ORTEP—a fortran thermal ellipsoid plot program. Technical Report ORNL-5138, Oak Ridge, 1976.
[16] P.R.E.C.F. Macrae, P. McCabe, E. Pidcock, G.P. Shields, R. Taylor, M. Towler, J. van de Streek, J. Appl. Cryst. 39 (2006) 453.
[17] R.D. Shannon, Acta Crystallogr. Sect. A32 (1976) 751–767.
[18] I.D. Brown, D. Altermatt, Acta Crystallogr., Sect. B: Struct. Sci B41 (1985) 244–247.
[19] A TGA was performed under airflow from room temperature to 1000 °C with a heating rate of 10 $Kmin^{-1}$ on a TGA Q500 apparatus for biphenylenediphosphonic acid. Total weight lost at specific temperatures are given: biphenylenediphosphonic acid (250 °C 0.72 %, 300 °C 4.24%, 330 °C 6.61%), lithium biphenylenediphosphonate (300 °C 0.18%, 330 °C 1.61%).
[20] R. Murugavel, N. Gogoi, Bull. Mater. Sci. 32 (2009) 321–328.
[21] C.N.R. Rao, S. Natarajan, A. Choudhury, S. Neeraj, A.A. Ayi, Acc. Chem. Res. 34 (2001) 80–87.
[22] S. Natarajan, A.K. Cheetham, Chem. Commun. (1997) 1089–1090.
[23] D. Tanaka, S. Kitagawa, Chem. Mater. 20 (2008) 922–931.
[24] R. Vaidhyanathan, S. Natarajan, A.K. Cheetham, C.N.R. Rao, Chem. Mater. 11 (1999) 3636–3642.
[25] H.-H. Song, L.-M. Zheng, Z. Wang, C.-H. Yan, Xin, Inorg. Chem. 40 (2001) 5024–5029.
[26] L. Liu, J. Li, Z.-G. Sun, D.-P. Dong, N. Zhang, X. Lu, W.-N. Wang, F. Tong, ZAAC 636 (2010) 247–252.
[27] X. Lu, J. Li, Z.-G. Sun, D.-P. Dong, R.-N. Hua, N. Zhang, L. Liu, F. Tong, W.-N. Wang, ZAAC 635 (2009) 2617–2621.